International Journal of Robotics and Control Systems
Vol. 4, No. 3, 2024, pp. 1135-1157
ISSN 2775-2658
http://pubs2.ascee.org/index.php/ijrcs

Optimized Fault Detector Based Pattern Recognition Technique to Classify and Localize Electrical Faults in Modern Distribution Systems

Chandra Sekhar Mishra [a,1], Ranjan Kumar Jena [a,2], Pampa Sinha [b,3], Kaushik Paul [c,4], Mohamed Metwally Mahmoud [d,5], Mohamed F. Elnaggar [e,f,6,*], Mahmoud M. Hussein [d,g,7], Noha Mohammed Anwer [h,8]

[a] Odisha University of Technology and Research (Bhubaneswar) formerly Known College of engineering and technology (CET), India
[b] School of Electrical Engineering, KIIT Deemed to be University, Bhubaneswar, India
[c] Department of Electrical Engineering, BIT Sindri, Dhanbad 828123, India
[d] Electrical Engineering Department, Faculty of Energy Engineering, Aswan University, Aswan 81528, Egypt
[e] Department of Electrical Engineering, College of Engineering, Prince Sattam Bin Abdulaziz University, Al-Kharj 11942, Saudi Arabia
[f] Department of Electrical Power and Machines Engineering, Faculty of Engineering, Helwan University, Helwan 11795, Egypt
[g] Department of Computer Technology Engineering, Technical College, Imam Ja'afar Al-Sadiq University, Baghdad, Iraq
[h] Electrical Power and Machines Engineering Department, High Institute of Engineering and Technology, Luxor, Egypt
[1] chandrasekharmishra1106@gmail.com; [2] ranjankjena@gmail.com; [3] pampa.sinafel@kiit.ac.in;
[4] ushik.ee@bitsindri.ac.in; [5] metwally_m@aswu.edu.eg; [6] mfelnaggar@yahoo.com; [7] mahmoud_hussein@aswu.edu.eg;
[8] nohaanwer69@yahoo.com
*Corresponding author

ARTICLE INFO

Article history
Received May 11, 2024
Revised June 26, 2024
Accepted July 05, 2024

Keywords
Artificial Neural Networks;
Discrete Wavelet Transform;
Niche Binary Particle Swarm Optimization;
Modern Distribution Systems;
Control Systems

ABSTRACT

This research presents a method that integrates artificial neural networks (ANN) and discrete wavelet transform (DWT) to identify and classify faults in large power networks, as well as to pinpoint the zones where these faults occur. The objective is to enhance reliability and safety by accurately detecting and categorizing electrical faults. To manage the computational demands of processing the extensive and complex data from the power system, the network is divided into optimal zones, each made visible for fault detection. Niche Binary particle swarm optimization (NBPSO) is employed to place the fault detectors (FD) in each zone. This allows for precise measurement of fault voltage and current phasors without significant cost. The ANN module is tasked with identifying the fault area and locating the exact fault within that zone, as well as classifying the specific type of fault. Discrete Wavelet Transform is used for feature extraction, and a phase locked loop (PLL) is used for load angle computation. The proposed method's validity has been tested on the IEEE-33 bus distribution network.

1. Introduction

In modern power distribution systems, the prompt and accurate detection and localization of electrical faults are critical for maintaining system reliability and safety. Electrical faults, which can be caused by various factors such as equipment failures, weather conditions, or operational errors, pose significant challenges. They can lead to power outages, equipment damage, and safety hazards [1]-[4]. Therefore, developing advanced techniques for fault detection and classification is essential for efficient power system management. Traditional fault detection methods often struggle with the complexities and scale of modern power networks. They may involve significant computational overhead and may not provide the desired accuracy or speed in identifying and localizing faults. To address these challenges, this research proposes an innovative approach that leverages artificial neural networks (ANN) and discrete wavelet transform (DWT) to improve the detection, classification, and localization of faults in power distribution systems [5]-[7].

Transmission lines are vital components of electrical power systems, connecting generation centers to load centers. An electrical fault, a malfunction in wiring or appliances, can lead to power outages, damaged electronics, and even pose safety risks to humans, birds, and animals. Rapid detection and isolation of such faults are crucial to minimizing disruption [8]-[11]. Several methods for fault detection and localization in transmission lines have been explored and reviewed in various studies. Traditional methods often involve mathematical and predictive models enabled by advancements in computing technology. For instance, an ANN-based defect detector has been proposed for fault classification, though it did not address fault location accurately. Hybrid strategies combining techniques like support vector machine (SVM), genetic algorithm (GA), and DWT-extreme learning machine (DWT-ELM) have also been surveyed and compared [12]-[15]. In one study, a case using ANN to detect faults in a protective zone reported an accuracy of 78.82%. Researchers have also employed mathematical modeling and optimization techniques, such as teaching learning based optimization (TLBO) and harmony search (HS), to locate faults in a two-end transmission line model. Moreover, nonlinear loads injecting harmonics into the system can distort voltage and current waveforms, necessitating techniques to identify harmonic current sources for reliable power delivery [16]-[18]. Innovative methods, such as using ANN with directed relay systems for smart grid protection, have been proposed. These systems employ either a centralized controller receiving data from all protection devices or a zone controller facilitating communication between peer protection devices along the line. This approach eliminates the need to reconfigure protection settings when grid layouts change [19]. Another study utilized MATLAB to test a 14-bus system, using ANN trained with back-propagation to detect and classify faults, achieving a mean square error (MSE) within acceptable ranges and high precision various techniques, including the hubbard-stanovich (HS) transform and radial basis function-ANN (RBFANN), have been mentioned for FD and localization [20]. Time Frequency Analysis plays a key role in feature extraction, calculating standard deviations and energy changes over configurable windows. RBFANNs classify faults using energy delta and standard deviation as inputs. Additionally, a combination of DWT and back propagation-ANN (BPANN) has been developed to locate faults in underground supply networks, utilizing high-frequency fault signal components for precise detection [21]-[23].

For fault distance estimation, decision tree regression (DTR) has been employed due to its resilience and faster training compared to other techniques like ANNs and SVMs. This method uses fault data to estimate fault location, showing robustness against various fault conditions and system characteristics. Digital relaying with fast discrete orthogonal S-transform (FDOST) and SVMs has been used to accurately locate faults under different conditions, even with noisy signals [24], [25]. SVM have also been utilized for fault detection and classification, requiring a database of detail coefficients from DWT-decomposed current and voltage signals for model training. The resulting models can effectively identify and classify faults along transmission lines. Additionally, methodologies involving phasor measurement units (PMUs) and Clark components have been developed to enhance fault detection and localization indices, reducing system noise and measurement errors [26]-[28]. In power systems, devices like STATCOM are essential for maintaining voltage stability and power quality. Techniques involving DWT analyze signals to detect faults, particularly in relation to STATCOM's role in reactive power control. Collecting and processing data from multiple points in the system helps identify fault conditions accurately, ensuring reliable power transmission [29]-[35].

The proposed method divides the power network into optimal zones to manage the extensive data efficiently. Within each zone, a fault detector (FD) utilizing niche binary particle swarm optimization (NBPSO) is employed. This approach allows for precise measurement of fault-related parameters, such as voltage and current phasors, while minimizing costs. The ANN module plays a crucial role in identifying the fault area and pinpointing the exact fault location within that area. Additionally, the ANN is capable of classifying the specific type of fault, providing valuable information for swift corrective actions. For feature extraction, DWT is applied, which effectively captures the transient characteristics of faults. Furthermore, a phase locked loop (PLL) is used for load angle computation, enhancing the accuracy of the fault detection process. The proposed method has been validated using the IEEE-33 bus distribution network is presented in Fig. 1, demonstrating its effectiveness and reliability in real-world scenarios. This paper outlines the methodology, implementation, and validation of this advanced fault detection technique. The following sections will discuss the literature review, methodology, experimental setup, results, and conclusions, providing a comprehensive overview of the research and its implications for power distribution systems.

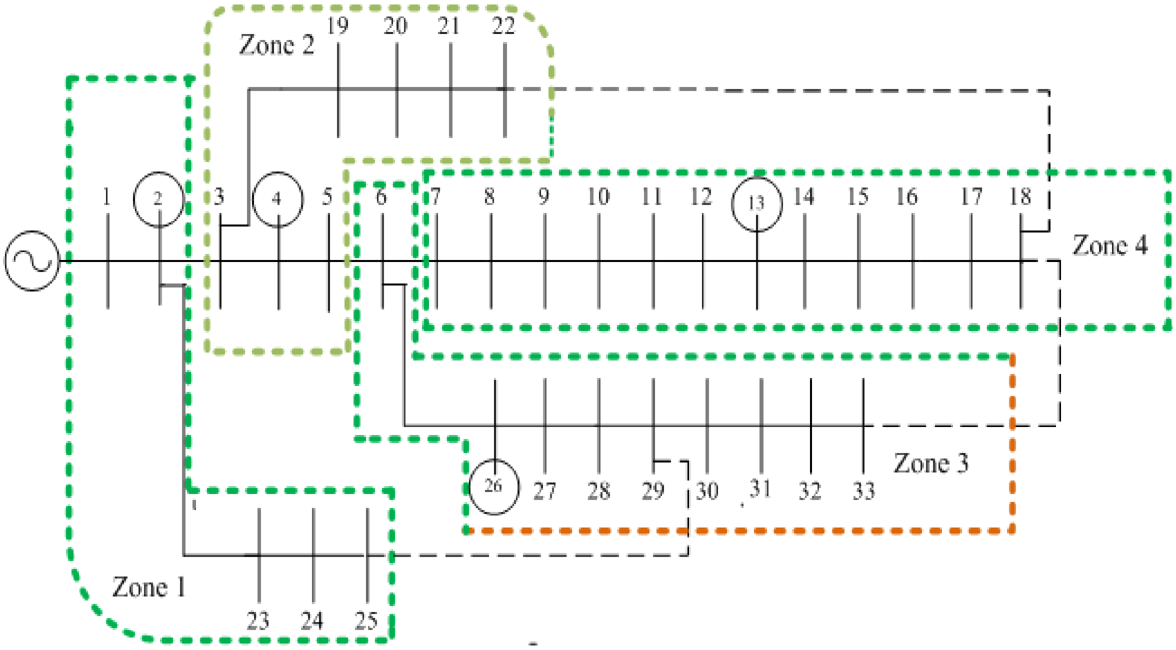

Fig. 1. Schematic representation of zones divisions in IEEE 33 bus system

2. Power System FD and Classification Methodology

The proposed algorithm is divided into two primary sections: fault zone detection and fault classification. The flowchart of this algorithm is depicted in Fig. 2. The process begins with the initialization phase, where the power system is divided into zones, and FDs are strategically placed within these zones using the NBPSO algorithm. These FDs continuously monitor and record three-phase voltages, currents, and load angles. DWT is then applied to these recorded measurements to extract specific coefficients from the voltage and current waveforms. Additionally, the ANN pattern recognition technique is employed to detect and categorize fault zones within the power system [36], [37]. A detailed description of the FD and classification procedure is provided below [38].

2.1. Selection of Optimal Zones

Transmission lines are critical for transporting electrical energy over long distances, connecting power plants to consumers [39]. In this model of the electrical grid, buses serve as nodes, and power cables serve as branches. The proposed approach for fault localization leverages the NBPSO algorithm and incorporates network topology information. When a bus's observability is enabled, the controller can take voltage or current readings from the bus and use them as inputs to train an ANN. The fault locator is positioned at bus p,p, making it observable. For a bus to be considered observable, it and all buses it connects to must meet the observability criteria. The topological FD (TFD) matrix for a bus incident is constructed, where node elements are represented as columns and branches as rows. The placement of FDs within the network topology-based TFD is determined as follows [40]-[42]:

"FD(p,p)=1"; for all buses in the power system

"FD(p,q)=1"; "If the buses p and q are connect"

"FD(p,q)=0"; "If the buses p and q are not connected"

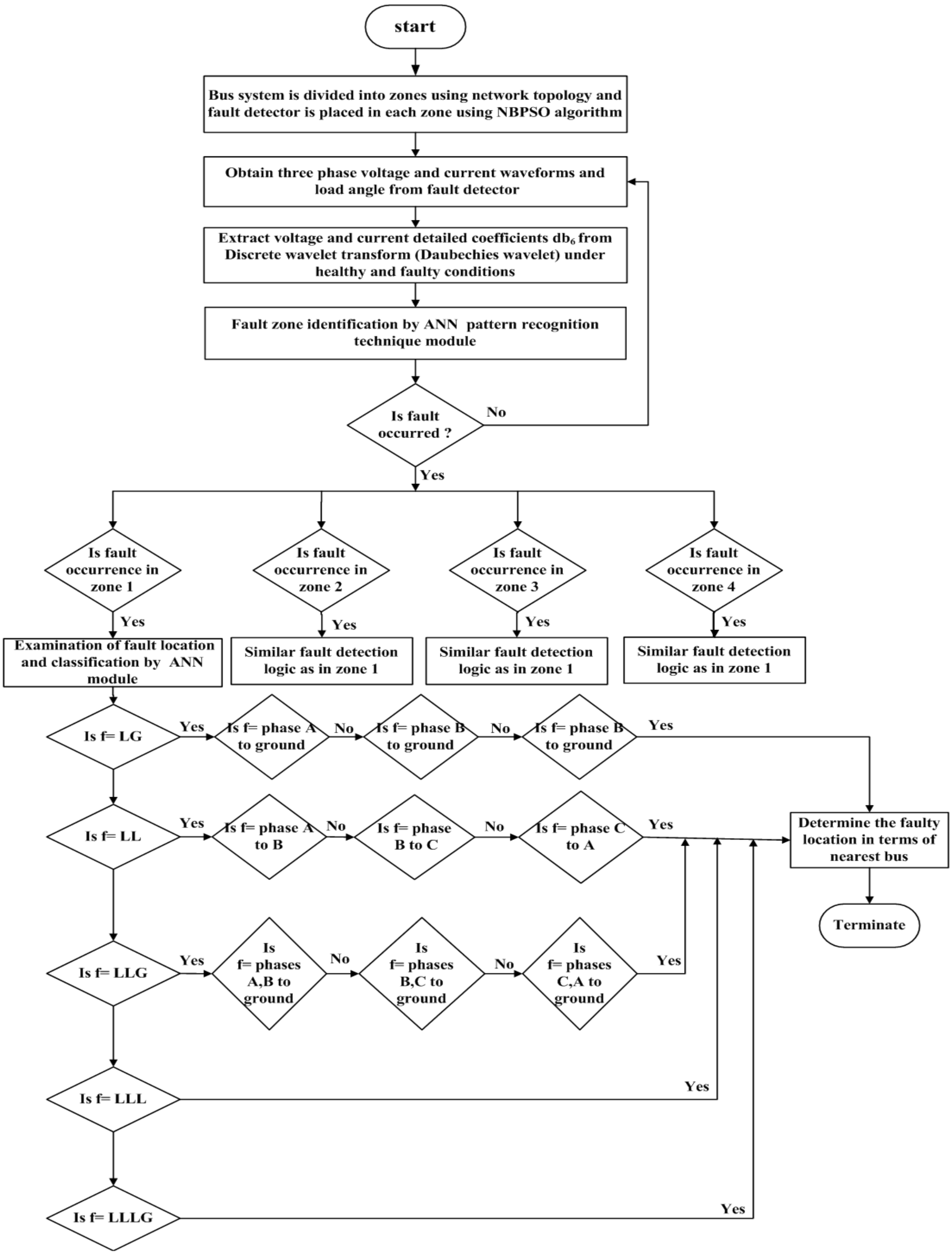

Fig. 2. Complete flowchart for the proposed fault identification and classification

The flowchart in Fig. 3 shown the approach for the optimal selection of zones and makes the system observable. Further, the placement of FD at each zone will be discussed. This flowchart illustrates the approach for optimal zone selection, ensuring system observability. The subsequent placement of FDs within each zone is then discussed in Table 1.

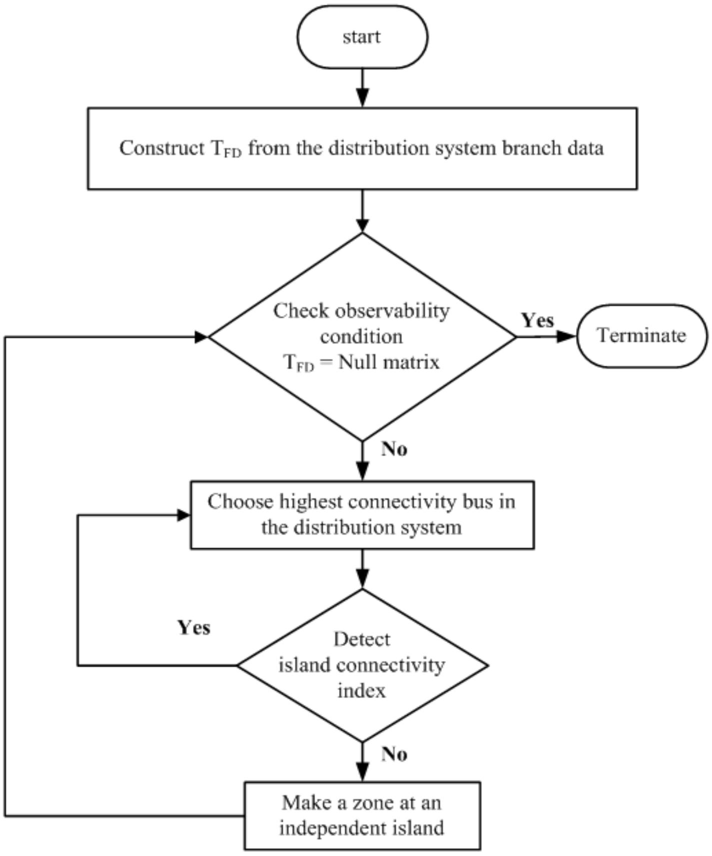

Fig. 3. Flowchart of the Selection of optimal zones approach

Table 1. IEEE 33 bus zone protection

Zone	Bus Numbers IEEE 33 BUS
Zone A	1 , 2 , 3 ,19 , 20 , 21, 22 , 23 , 24 , 25
Zone B	4,5,26,27,28,29,30,31,32,33.
Zone C	7,8,9,10,11,12,13,14,15,16,17,18

2.2. FD and Categorization Procedure

In [43], the authors have formulated a new approach for the harmonic source identification in the power system framework that deals with the wavelet transform. The approach has been inspired by the active power harmonic analysis based on the analysis of the detail or harmonic active power in the wavelet domain [44]. Based on the DWT, the mathematical representation of the active power P, can be represented as:

$$P = \frac{1}{T}\int_0^T v(t).i(t)dt \tag{1}$$

Here P can be segregated into components which are approximate (P_{app}) and detail power (P_{detj}). Thus, P can be represented as:

$$P = P_{app} + P_{detj} \tag{2}$$

where,

$$P_{app}=\frac{1}{T}\Sigma C_{jo,k}C'_{j0,k} \tag{3}$$

$$P_{detj}=\frac{1}{T}\sum_{j\geq j0}\sum_{k} d'_{j,k}\ d_{j,k} \tag{4}$$

Here represents the, Here in Equations (3), (4), the DWT coefficients related to the current and voltages are denoted as $C_{j0,k}$, $C'_{jo,k}$ respectively corresponding to the scaling level $j0$ and the level of wavelet decomposition is denoted as j. $d_{j,k}$, $d'_{j,k}$ represented in Equation (4) resembles the DWT coefficient for current and voltage respectively at k^{th} sample. In Equation (5) and Equation (6), The RMS values of the voltage and current signals corresponding to specific frequency band are marked as V_j and I_j which resembled the detailed voltage (V_{det}) and detailed current (I_{det}), respectively.

$$V_{detj}=\frac{1}{\sqrt{T}}\sqrt{\sum_{j\geq j0}\sum_{k}d'} \tag{5}$$

$$I_{detj}=\frac{1}{\sqrt{T}}\sqrt{\sum_{j\geq j0}\sum_{k}d} \tag{6}$$

$$C'_{j0,k}=\langle v(t),\varphi j_{j0,k}\rangle\ ,\ d'_{j0,k}=\langle v(t),\psi j_{j0,k}\rangle \tag{7}$$

$$C_{j0,k}=\langle i(t),\varphi j_{j0,k}\rangle\ ,\ d_{j0,k}=\langle i(t),\psi j_{j0,k}\rangle \tag{8}$$

In Equations (7) and (8), and the scaling function is represented as $\varphi_{j0,k}$, and $\psi_{j,k}$ represents the wavelet basis function respectively [43]. Formula for detail active power at level 1 (P_{det1}) is given as:

$$P_{detj}=\frac{1}{T}\sum_{j\geq j0}\sum_{k} d'_{1,k}\ d_{1,k} \tag{9}$$

In Equation (9), the DWT coefficient for current is represented as $d_{1,k}$ and for voltage is represented as $d'_{1,k}$ corresponding to the 1^{st} decomposition level and k^{th} sample.

Pdet1 resembles the element energetic electricity at level 1, that is associated to a targeted node that determines whether or not area of the source of harmonic pollutants is located on the downstream or upstream considering the node because the reference. At a particular factor inside the considered device, if the fee of Pdet1 is high-quality, then it signifies that the harmonic energy has been acquired from the upstream facet with respect to the point of measurement. similarly, whilst the price of Pdet1 resembles a negative signal then it's far taken into consideration that the harmonic electricity is obtained from the downstream aspect. In case while there may be a couple of harmonic supply are present then a conflicting state of affairs arises. In such state of affairs, the identification of the stronger harmonic source is done via determining the pollution power (DP) degree of the source. The source that is highlighting higher value of DP is handled as the dominant dealer of harmonics. The dominant source of harmonic pollution region can be determined deliberating the signs of the element electricity for the state of affairs while single nonlinear load or a couple of nonlinear loads are present.

2.3. Specific Harmonic Source Identification Based on the Selection of Signature Harmonic Frequency

In well known principles, the source's characteristic harmonic information is utilized because the fundamental idea of governing the detection of the form of harmonic generating source. Such statistics is without problems handy for usually used distribution device loads. The strength digital hundreds which can be taken into consideration to be the primary producers of harmonics in power structures framework, normally produce ordinary harmonics. This situation can be almost observed in case of a 6-pulse converter that bears sizable quantity of 5th and 7th harmonic additives and each eleventh and thirteenth additives of the harmonics are dominant for 6 pulse converters in addition to for 12 pulse converters. it's also visible that triple harmonics are present in case of the transformer thrilling present day. consequently, it could be located that based on the characterizing harmonics the identification of a specific traumatic load can finished. The proposed method, the wavelet analysis of the active power signal at detail level 1 has been utilized to search the frequency. The information related to the desired harmonic power is achieved based upon the adjustment performed in the sampling frequency. In this paper, the optimum sampling frequency can be described as the sampling frequency that facilitates the extraction of the information related to the corresponding harmonic information at detail level 1. Obviously, the optimum sampling frequency will depend upon the frequency of the signal to be extracted and also on the central frequency of the mother wavelet chosen which is shown in Table 2.

Table 2. Comparative analysis at 1st level of decomposition between Pseudo and sampling frequency

Specific Harmonic	Captured power frequency (Hz)	Sampling frequency (Hz)
3rd	300	877
5th	500	1461.56
7th	700	2046.185
9th	900	2630.8
11th	1100	3215.43
13th	1300	3800

2.4. Optimum Sampling Frequency for Finding out the Different Types of Harmonics Generating Source

The frequency information from the coefficient extracted at the j^{th} decomposition level in case of the wavelet decomposition can be represented as:

$$F_{psj} = \frac{F_c F_j}{2^j} \tag{10}$$

where, In Equation (10), the pseudo frequency at j^{th} level is given as F_{psj}, F_s resembles the sampling frequency and the frequency of mother wavelet i.e. central frequency related to the selected wavelet is represented as F_c [23]. The mother wavelet db^{10} has been used in this study as this has been found to be the most suitable mother wavelet for steady state power system distorted waveform analysis [45]. F_{psj} resembles the frequency band around the frequency F_{psj} even it has a single frequency value. The computation of the sampling frequency can be done considering the information related to the pseudo frequency that have been fetched regarding the signature harmonics of the voltage/current signal. The proposed approach portrays the search of the characterizing frequency bands based on the decomposition of the power signal for the distribution system loads. The voltage and current have 50 Hz as the fundamental frequency, and the active power signal exhibits a 100 Hz frequency. Accordingly, for the third harmonic the frequency of the active power component is 300 Hz. Thus, the determination of sampling frequency in case of the fundamental active power extraction at the level 1 of the discrete wavelet transform can be represented as:

$$Fs = \frac{2 \times Fps_j}{0.6842}\ Hz \tag{11}$$

The pseudo frequency, and the sampling frequency corresponding to each harmonic level has been shown in Table 1 for Daubesis 10 (db^{10}) mother wavelet and the decomposition at the first level. The frequency band estimation included in a wavelet analysis with specific frequency F_{psj} of level j, is represented as:

$$F_{psj} = \frac{(m+1)F_s}{2^{j+1}} \; ,j = 1, J-1 \tag{12}$$

where In Equation (12), F_s is denoted as the sampling frequency and J is the last decomposition level. Range of m is denoted as $m=0, 1, ^{j-1}$ and m=0, 1 for DWT [46]. An experiment has been conducted for a network energized with a non-sinusoidal voltage source which has all odd harmonics up to 19th order in order to further verify the above condition. Because the network's loads are considered to be linear, the present. Table 3 shows the proportion of harmonic power computed by P_{det1} at sampling frequencies of 877 Hz, 1461 Hz, and 3800 Hz. These frequencies resemble the specific pseudo frequencies of 3rd, 5th, and 13th harmonic powers, respectively. At a sampling frequency of 1461 Hz, which corresponds to the 5th harmonic power, P_{det1} so it can determine the 5th harmonic power. P_{det1} calculates 85.26% of 3rd harmonic power, 83.24% of 7th harmonic power, and 20.46% of 9th harmonic power at this sampling frequency, with the influence of other harmonic powers minimal. Similarly, at 877 Hz sampling frequency, P_{det1} only records 100% of the 3rd harmonic power and 20% of the 5th harmonic power. Table 3 also shows the contributions of the harmonic powers on P_{det1} at 3800 Hz sampling frequency. The above analysis serves as the foundation for the harmonic source detection strategy in our suggested method. The main concept deals with the pseudo frequency selection that aids in the detection of the source. Subsequently, the sampling frequency must be selected so that the extraction of the pseudo frequency component can be done at level 1 of wavelet. The characteristic pseudo frequency must be chosen with care in order to encompass the bulk of the harmonics created by the harmonic generator and gather their contributions to the extracted coefficient for the purpose of detecting the harmonic source. As a result, the sample frequencies must be modified based on the defining harmonics of the targeted harmonic generating sources, as various harmonic sources may have different characteristics frequencies.

Table 3. Different values of pdet1 at various sampling frequencies

Harmonic order	F_s =1461 Hz	F_s = 877 Hz	F_s = 3800 Hz
Fundamental	1.05	3.9	0.12
3rd order Harmonic	86.5	100	0.76
5th order Harmonic	100	19.5	1.96
7th order Harmonic	86.7	-	5.89
9th order Harmonic	19.78	-	19.89
11th order Harmonic	-	-	83.6
13th order Harmonic	-	-	100
15th order Harmonic	-	-	82.6
17th order Harmonic	-	-	42.5
19th order Harmonic	-	-	12.5

3. Proposed Fault Diagnosis and Detection Method at Each Zone

The fault condition test signal changes its amplitude and frequency; eventually, the entropy of the test signal also changes its value. Entropy also determines the type of fault in the distribution system. In the proposed algorithm, phase currents and ground current signals $(i_a, i_b, i_c and i_g)$are the test signals for FD. The value of ground current is mathematically represented in Equation (13) [47],

$$i_g = i_a + i_b + i_c \tag{13}$$

The proposed method calculates the entropy of each phase current signal before and after the fault condition. The flowchart of the proposed method is shown in Fig. 4. $suma, sumb, sumcandsumg$ represents the entropy values of current signals. The maximum and minimum values of these sum of entropy values are calculated to compare with threshold values [48].

$$max\,1 = max(suma, sumb, sumcandsumg) \tag{14}$$

$$max\,2 = immediate(max\,1) \tag{15}$$

$$min\,1 = min(\,suma, sumb, sumcandsumg) \tag{16}$$

The threshold values TH1, TH2 and TH3 sets according to the system for FD and classification. These threshold values compare min and max values and set rules for fault type classification. The following rules are [48]:

No-Fault Condition: $\frac{min}{sumg\frac{max\,2}{min}}$

L-L Fault: $\frac{min}{sumg\frac{max\,2}{min}}$

L-L-L-G Fault: $\frac{min}{sumg\frac{min}{sumg}}$

L-G Fault: $\frac{min}{sumg\frac{min}{sumg}}$

L-L-G Fault: $\frac{min}{sumg\frac{min}{sumg}}$

Niching technique has evolved by incorporating the interaction of competitive behaviour of animals and other species in a situation where the possessions are partial. Where Niches is identified as partitions of situation (or environment), while species can be interpreted as the division of population contending in the situation. Niching systems is categorized by two diverse methods: "parallel and sequential niching" [49]. "Parallel niching" technique identifies and maintains various "niches" in population simultaneously. "Sequential niching technique implements multiple solutions by iteratively applying niching to a problem space, while marking a potential solution at each iteration to ensure that search efforts are not duplicated".

"Niching algorithms" present actual substitutes to unimodal optimization techniques in multi model domains. Difficulties with multi model solutions spaces, such as resolving equations of the systems and collaborative neural networks, can be beneficial rather than optimization approaches, which explicitly undertake more than a single solution, and lead to more efficient optimization. NBPSO is popular with its multidimensional search and is capable of developing a range of system equation solutions. It uses a "local search algorithm" to build "sub-swarms" to find the finest Gbest position in the "swarm". The procedure overlays the "initial partial swarm" with the harming distance. The objective function is distinct by fault detector. The purpose of "NBPSO algorithm" is to obtain best solution redundancy and fulfil the constraints to obtain observability of distribution system.

Let the FD "placement vector" "S" as defined by:

S(p)=If FD "placed at bus" p; otherwise

The "NBPSO problem is formulated as follows"

$$\text{“}Minimize\text{”}\; W1M1 + W2M2 \tag{17}$$

Constraints subjected to TFDST≥ U "Where TFD is binary incidence matrix of n bus system and given as unity vector U= (n×1). W1 and W2 are weights to compare magnitudes M1 and M2."

$$\text{“}M1 = STs\ represents\ the\ total\ number\ of\ FD's\ in\ the\ system\text{”} \tag{18}$$

$$\text{“}M2 = \;((N - TFDS)T * (N - TFDS))\text{”} \tag{19}$$

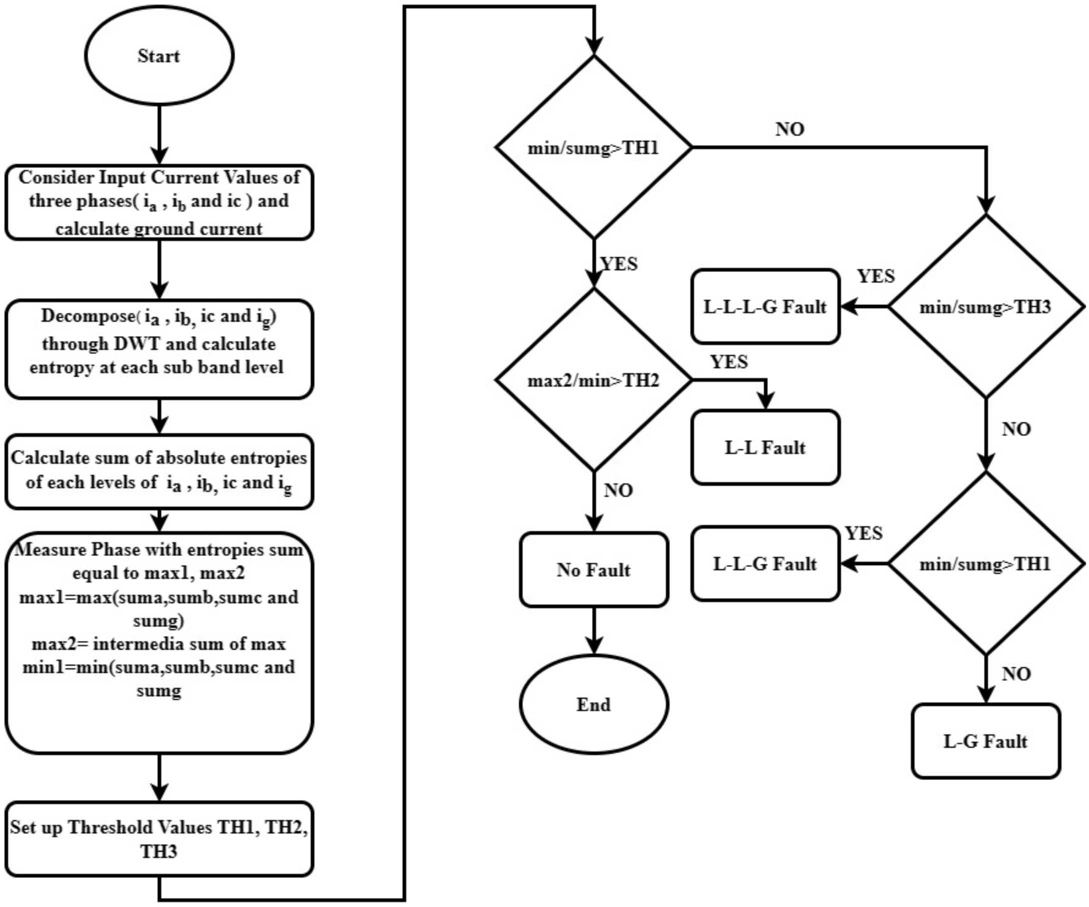

Fig. 4. Flowchart of proposed fault diagnosis method

where N represents redundancy matrix of size (n×1), the elements are in the N matrix has set to 3 if the redundancy level of the system is 2. TFD S is given by the observability of the bus done by the placement of FD. (N-TFDS) gives the variance of the observed and anticipated number of a bus observed. Therefore, by the FD placement in the system the function M2 maximizes the redundancy.

This algorithm has attained the convergence and found the output in the function of fault detector at each zone. Further DWT will be discussed to obtain the approximate coefficient. The flowchart is explained in Fig. 5.

4. ANN for Pattern Recognition Technique

ANN is a computational model, specifically based on structures and features of biological neural networks. An ANN work with a large nonlinear statistical data that can build a complex relationship between inputs and outputs, makes it's robust in nature, because of its high accuracy in prediction where the output is very close to the actual value. Its accuracy of prediction made the ANN to be utilized in various applications such as aerospace, speech telecommunications, protection systems etc. [50]. The training process of ANN involves training of the neurons to update set of weights for mapping the pattern of input to outputs. An ANN structure has an input layer, hidden layer (there can be greater than 1) and the output layer. The hidden layer can extract some of the essential patterns from the inputs and passes it onto the subsequent layer to see. It makes the network faster and efficient [48].

4.1. ANN-FD Module

By employing the pattern-recognition capabilities of ANNs, we can more accurately identify transient and fault states in the power grid. It can also tell the difference between a single-phase and three-phase power failure. The three-phase voltage and current root-mean-square values, feature extraction from discrete wavelet transform at db6 frequency, and load angle computed from phase-locked loop are among the nine inputs into the ANN module under consideration. Table 4 displays the basic layout of an ANN used for defect identification.

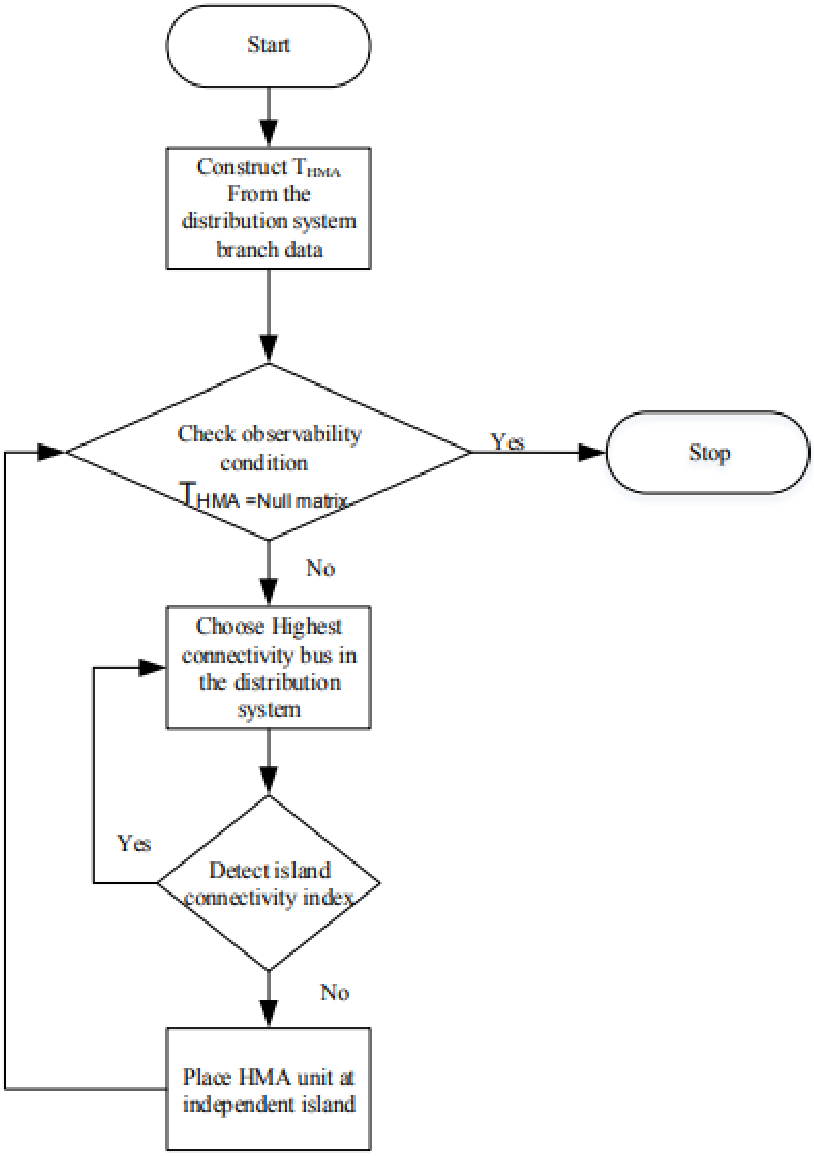

Fig. 5. Flowchart of NBPSO method

Table 4. ANN configuration network for zone detection

No. of Inputs	No. of Hidden Layers	No. of Outputs	ANN Model
9 (“VR, VY, VB,IR, IY, IB,Vco, Ico , ø”)	10	No. of zones in the distribution system	Two-layer feed forward neural network with sigmoid hidden and softmax output neurons

The output of the ANN module 1 intended to specify which fault occurrence zone. This module has developed to provide the output in the case of fault occurrence in the distribution system. The outputs have characterized by the binary coding of zone 1-4 to the correct input pattern [49]. Table 5 has represented the way of binary coding with the logic (1) and logic (0). The binary coding has assigned with each fault occurred zone as logic (1) or if not with logic (0). By using this approach, the ANN module 1 has provided training in accuracy for classifying the correct fault zone.

Table 5. Binary outputs coding of the ANN module 1

Fault occurrence zone	Result 1	Result 2	Result 3	Result 4
Zone no.1	1	0	0	0
Zone no. 2	0	1	0	0
Zone no. 3	0	0	1	0
Zone no. 4	0	0	0	1

4.2. ANN Fault Classification Module

The ANN module 2 is utilized for fault classification and uses the 9 inputs. The ANN utilizes back propagation algorithm with 10 hidden layers shown in Table 6. The output class is contained of five outputs as power system short circuit faults “L-G, L-L, L-L-L, L-L-G and L-L-L-G”.

Table 6. 10 hidden layers of ANN

No. of Inputs	No. of Hidden Layers	No. of Outputs	ANN Model
9 (“VR, VY, VB,IR, IY, IB,Vco, Ico , ø”)	10	5 (“L-G, L-L, L-L-L, L-G & L-L-L-G”)	The network is a two-layer feedforward neural network with sigmoid hidden and softmax output neurons.

The ANN module 2 outputs indicate the fault classification, which is linked to the correct input pattern. The outputs are characterized as logic (1) or (0) as in the form of binary coding given in Table 7. The output indicates either logic (1) if particular fault has occurred or it gives logic (0). In this way, the ANN module 2 has carried out the correct logic on each fault classification.

Table 7. Binary coding outputs of ANN module 2

Fault occurrence zone	Output 1	Output 2	Output 3	Output 4	Output 5
L-G	1	0	0	0	0
L-L	0	1	0	0	0
L-L-L	0	0	1	0	0
L-L-G	0	0	0	1	0
L-L-L-G	0	0	0	0	1

5. Results and Discussion

5.1. Investigations on the Studied System

In this section, IEEE 33 bus system is examined with the recommended technique. The proposed technique is studied in the context of the IEEE 33 bus system. The characteristics of the system are based on a 100 MVA rating and a 25 kV voltage. Fig. 1 depicts the updated IEEE 33 bus system with zoned division and FD location. Table 8 is shown for IEEE 33 distribution system simulation variables data set.

Table 8. IEEE 33 distribution system simulation variables data set

Variable parameter	Configurations
Fault Type	(LG, LL, LLL, LLG & LLLG)
Fault resistance	0.01Ω- 300Ω
Fault location(km)	(50,100,150,200,250,300,350,400) Zone1- Zone 4
Sampling Frequency	1200 Hz
Distribution system	Radial

The Proposed methodology works as following steps:

- The observability condition has checked in the system divided into 4 zones. The selection of buses by NBPSO from 2, 4, 13 and 26 in the respective zones (1- 4).
- The rms values of the phase voltages and phase currents, load angle from phase voltages have been collected from the fault detectors respectively under various fault occurrences.
- The voltage and current coefficients have extracted from DWT feature extraction at dB6 sampling frequency 1200 Hz.
- The input samples dimensions in 3,411 have been collected from each line in the IEEE 33 bus system. The FD provides 4 outputs of 1516 samples for a zone selection from zone 1-zone 4 are shown in Fig. 6.
- A two-layer feedforward network has been employed with a Line fault hidden layer of sigmoid transfer function, and the output layer take in softmax transfer function. The Preferred hidden neuron is set to 10. The number of target vector i.e. 4 has fault decided the number of output neurons.
- The ANN has used back propagation algorithm with 9 inputs, 10 hidden layers and 5 outputs as shown in Fig. 7 and Fig. 8. The ANN has been trained with supervised learning by theadjustment of weights of different fault conditions occurrence in the IEEE 33 distribution network.

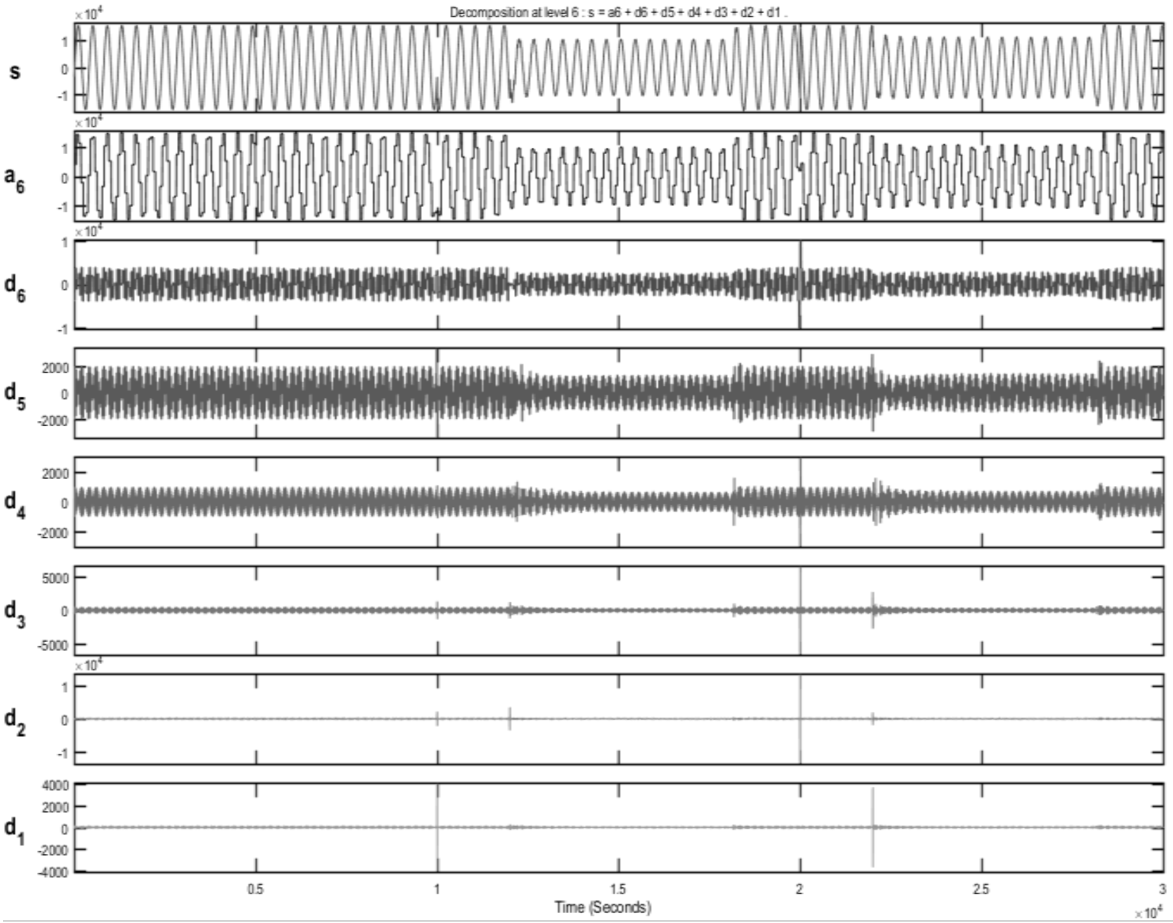

Fig. 6. Detecting an LG defect by DWT analysis of voltage

5.2. Performance Evaluation & Testing

The effectiveness of the proposed methodology has been evaluated for the zone detection and fault classification; the accuracies are calculated from the confusion matrix of the ANN modules 1&

2. The confusion matrix summarizes the ANN performance in classification between inputs and targets [51]. The features of the confusion matrix include training, validation, testing, and all confusion matrixes. The confusion matrix has shown be evidence for the number of mapped in green squares and unmapped samples in red squares to each classification. The individual classification percentage and the overall classification of each confusion matrix also have been specified in lower right blue squares [50]. The training of ANN has accomplished by which the result of the small least means square error as shown in the confusion matrix for fault classification and zone detection shown in Fig. 9 and Fig. 10. The training, validation, test and all confusion matrices have been generated from ANN module 1. Case study on IEEE 33 bus system with L-G fault occurrence at zone 2 shown in Fig. 11.

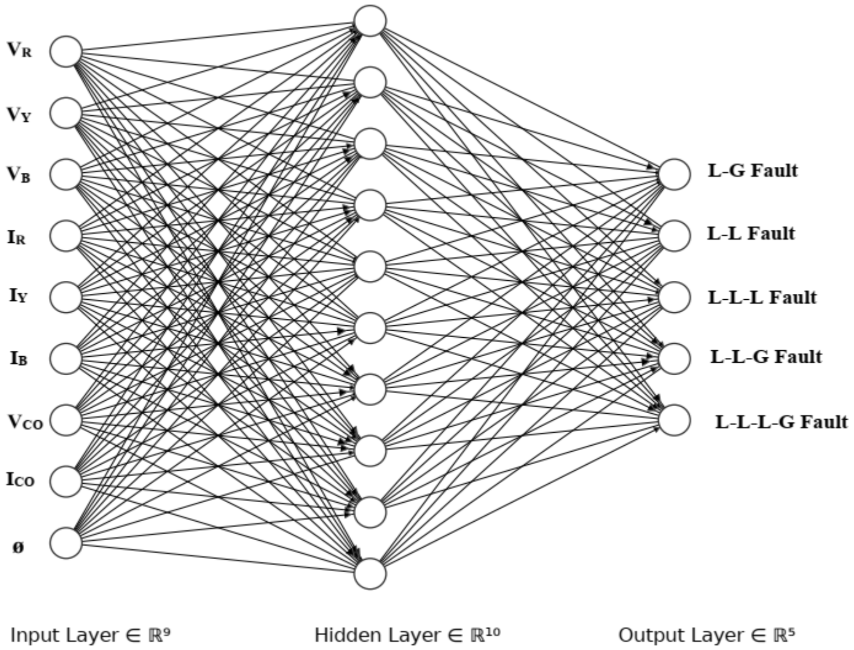

Fig. 7. ANN Module 1 configuration network for fault detection

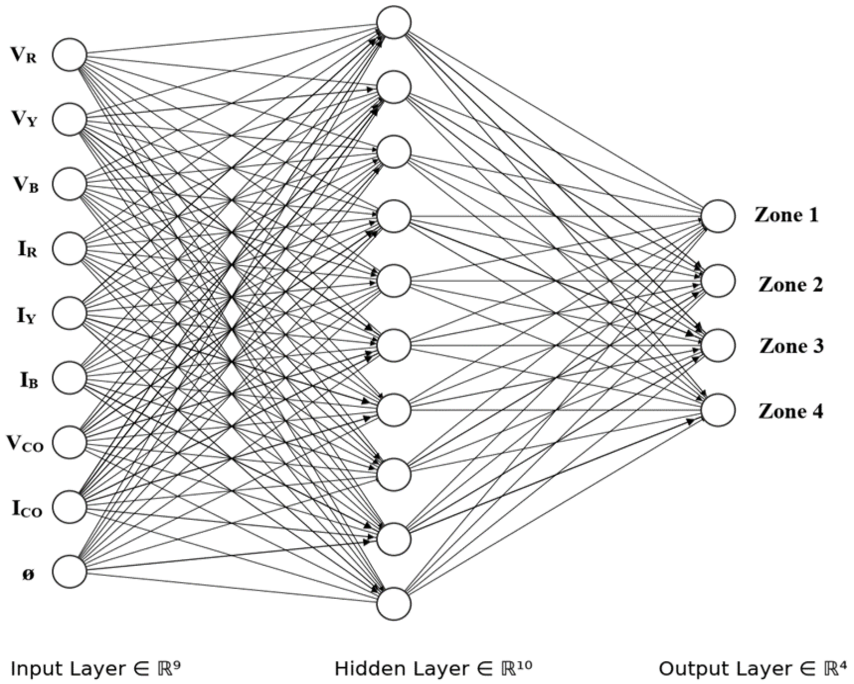

Fig. 8. ANN Mdoule 2 configuration network for fault classification

Vol. 4, No. 3, 2024, pp. 1135-1157

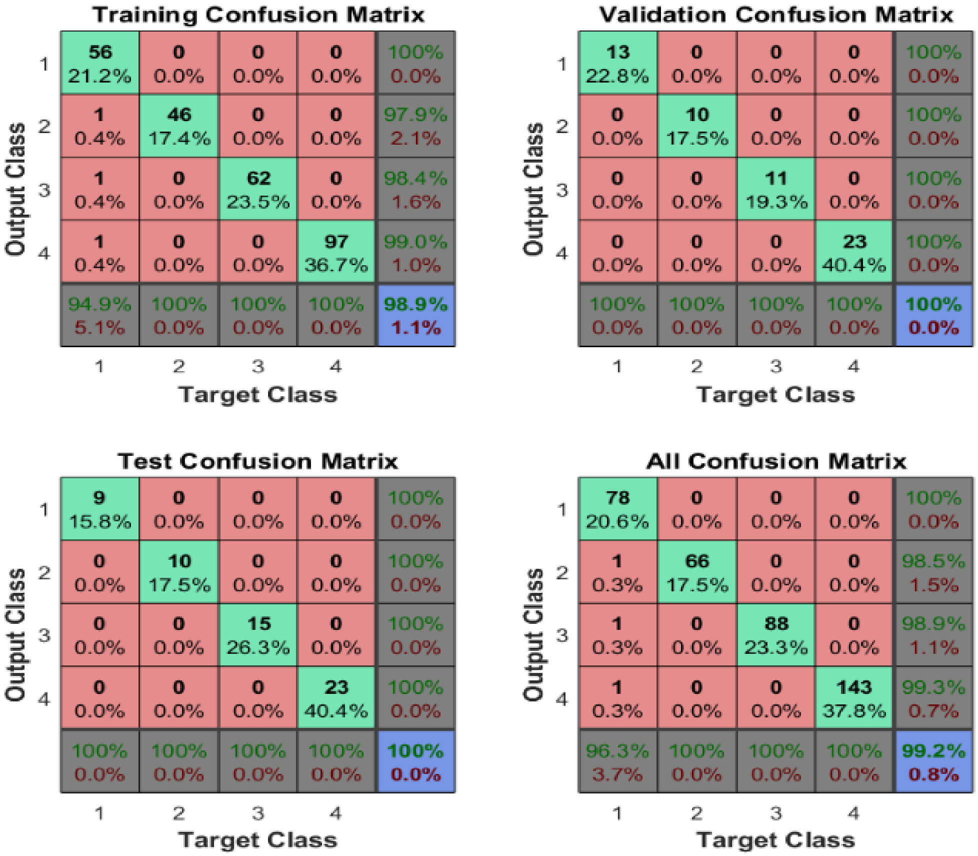

Fig. 9. Confusion matrix of ANN module 1 for FD

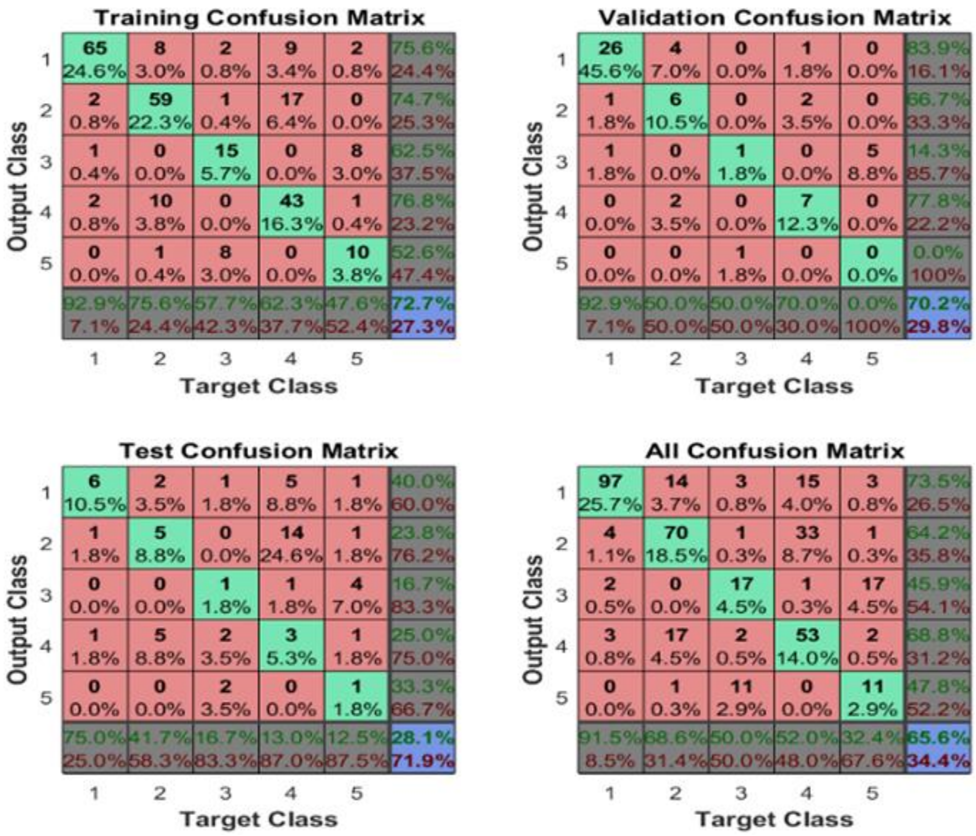

Fig. 10. Confusion matrix of ANN module 1 for zone detection

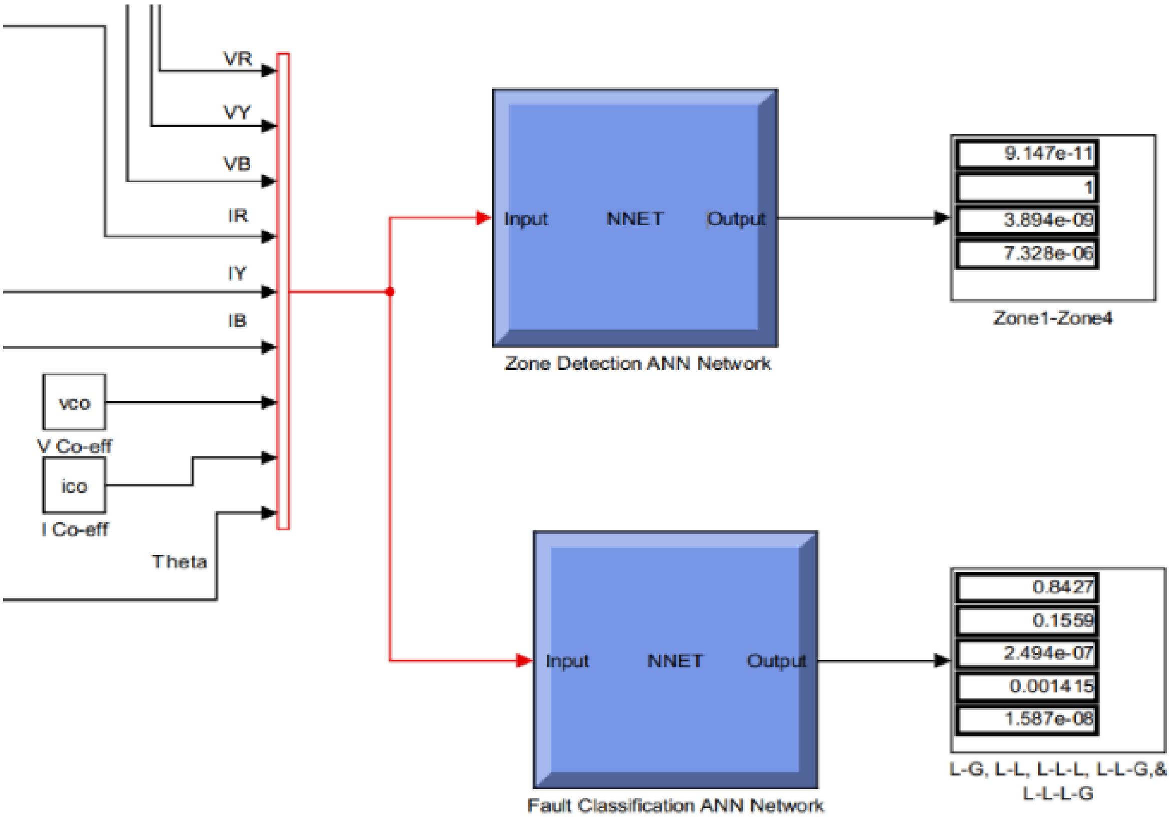

Fig. 11. Case study on IEEE 33 bus system with L-G fault occurrence at zone 2

5.3. Case study: L-G Short Circuit Fault Occurred Between Bus Number 5

The IEEE 33 bus balanced radial distribution test system at the suggested case site is given an L-G fault. The L-G fault is applied at a time interval ranging from 0.5 seconds to 0.7 seconds at the suggested site, and the required simulation work is carried out in MATLAB Simulink. The fault voltage signal has been logged, and it may be found shown in Fig. 12 (a). The fault current signal is shown in Fig. 12 (b). Smart meters positioned at bus numbers 5, 26, and 30 are responsible for the collection of the data for the failure signal. The non-fault signals are gathered at the other measurement devices that are still operational. This signal processing approach, which is based on the wavelet analysis decomposition, is used to deconstruct these signals. To solve this categorization issue, we looked at a total of 400 different samples. The quantity of these gathered data is rather substantial. Within this massive data set, only a select few data provide a more accurate interpretation of the signal. The process of selecting relevant features from a massive amount of data is referred to as feature detection. All the data were compared here with the actual value and the predicted value, and the results showed that the responses were more reliant on the data that had a high chi-square value.

ANNs have significant practical importance in classifying faults in various fields, including power systems. ANNs are adept at identifying complex patterns and relationships within data. In fault classification, ANNs can learn from historical fault data and their corresponding features to recognize patterns associated with different fault types. This enables accurate identification and classification of faults based on the input data. ANNs can adapt and learn from new data, making them suitable for fault classification in dynamic and evolving systems. As the system's behaviour changes over time due to different conditions and loads, ANNs can continuously update their classification capabilities. ANNs can automatically extract relevant features from raw data, reducing the need for manual feature engineering. This is particularly valuable in fault classification, where identifying relevant features can be challenging due to the complexity of the data. Fault patterns often involve nonlinear relationships between variables. ANNs are capable of modelling these nonlinear relationships, making them well-suited for capturing intricate fault patterns that might not be easily captured by traditional linear methods.

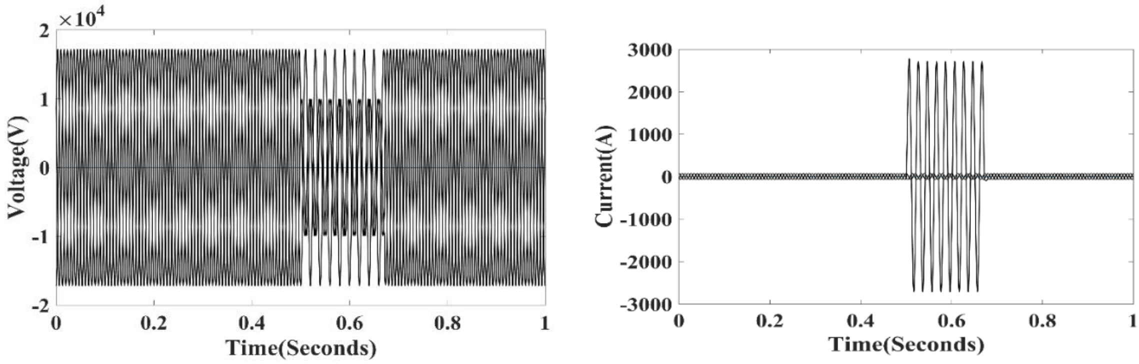

(a) (b)

Fig. 12. Voltage and current profile during LG fault

Trained ANNs can generalize their knowledge to classify unseen data accurately. This means that once an ANN has been trained on a sufficiently diverse dataset, it can classify new fault instances that it hasn't encountered during training. Fault Localization: ANNs can also be used for fault localization, helping to pinpoint the exact location of a fault within a system based on the observed data patterns. This can be crucial for efficient maintenance and quick restoration of servicesWhile some domain knowledge is necessary for designing and training ANN models, they can still achieve accurate fault classification without an exhaustive understanding of the underlying physical processes. This can be advantageous in cases where domain knowledge is limited or hard to acquire. ANNs can be designed to provide real-time or near-real-time fault classification, allowing for rapid response and mitigation of faults. This is especially important in critical systems like power grids, where timely actions can prevent widespread disruptions.

ANNs can handle data from various sources, including sensor readings, SCADA systems, and historical databases. This flexibility enables them to make use of diverse data streams for accurate fault classification. Reduced Human Intervention: Once trained, ANNs can operate autonomously, reducing the need for continuous human intervention in fault detection and classification processes. This can lead to improved efficiency and cost savings. These capabilities contribute to more reliable and efficient operation of complex systems, such as power grids, industrial processes, and communication networks. Table 9 shows that out of a total of 140 fault signal data, 137 of those data signals are accurately predicted and identified as belonging to Zone-B with an accuracy of 97.85 percent. It may be said that the categorization issue has an accuracy of 97.75 percent overall.

Table 9. Confusion matrix for case 1

N=400		**Predicted**			**CA (%)**
		BUS 5	**BUS 26**	**BUS 30**	
Actual	BUS 5	129	1	2	
	BUS 26	1	137	2	
	BUS 30	1	2	125	
					97.75%

5.4. Evaluation of the Proposed Method Using RTDS

For the experimental verification of the proposed method in the hardware platform, the authors have fed the IEEE 33 bus distribution system in the RTDS system. The considered model is simulated in PSim and the simulation has been carried out by utilizing Opal-RT RTS OP5600 chassis with RT lab form of 11.X. Voltage signals consequently produced by Opal-RT real-time test system, have been sent to IO cards ML605 to gather the required information. The assessment of the proposed strategy for location of HIF incorporates: i) impact of sampling rates; ii) impact of random noise iii) evaluation under DGs.

Sampling rates are very important for the measurement of voltage/ current signals utilized HIF detection technique. The digitization of voltage and current signals uses sampling rates in such a way that the signature of the signal should be intact. To assess the impact of the sampling rate for detecting HIF, four different sampling frequencies are considered i.e., 4 kHz, 10 kHz, 51.2 kHz, and 89.6 kHz have been chosen. The proposed strategy precisely identifies HIF at all sampling frequencies. The proposed methodology can detect HIF accurately at all sampling frequencies. But here particular to the industrial sampling frequency has been used i.e., 12.5 kHz for this work. The hardware model of the proposed scheme structure was presented in [5]. Fault in IEEE 33 Radial Distribution Under Noisy conditionThe detection of the HIF zone has been subjected to a noisy environment in hardware platform. Proper analysis of the noise impact is performed to evaluate the effectiveness of the projected approach. The signal-to-noise ratio (SNR) technically denotes noise, which is given by Equation (20).

$$SNR_{db} = 20\, log_{10}\left(\frac{X_{signal}}{X_{Noise}}\right) \tag{20}$$

Here the problem occurred between buses 5 and 16 in the presence of noise levels of 35dB, 25dB, and 10dB. TQWT signal processing technology is used to evaluate the fault signal, and fault data sets are gathered at smart meters positioned on buses 14 and 17. Levels 4 and 5 detail coefficients derived from the fault signal. The non-fault data sets are obtained from the smart meters located throughout the test system. The arc voltage at various noisy conditions is shown in Fig. 13 (a). In Fig. 13 (b), Kurtogram of noisy (10dB) has been shown where up to 13th order harmonics are visible.

Here 260 fault signals are given to the classification task. In 25 dB SNR noisy condition, out of 260 fault signals, 250 signals are categorized as zone 3 as its fault zone, with a classification accuracy of 99.24 %. The confusion matrix under 25 dB SNR noisy condition is shown in Table 10. In 15 dB SNR noisy condition, out of 260 fault signals, 258 signals are categorized as zone 3 as its fault zone with a classification accuracy of 99.23 %. The confusion matrix of case 3 under 10 dB SNR noisy condition is shown in Table 11. In Table 12, the proposed method outperformed all the existed methods in the literature, even though Tellegen's theorem and SWT+ANN have 100 % accuracy. They are limited to FD and no noise condition is considered.

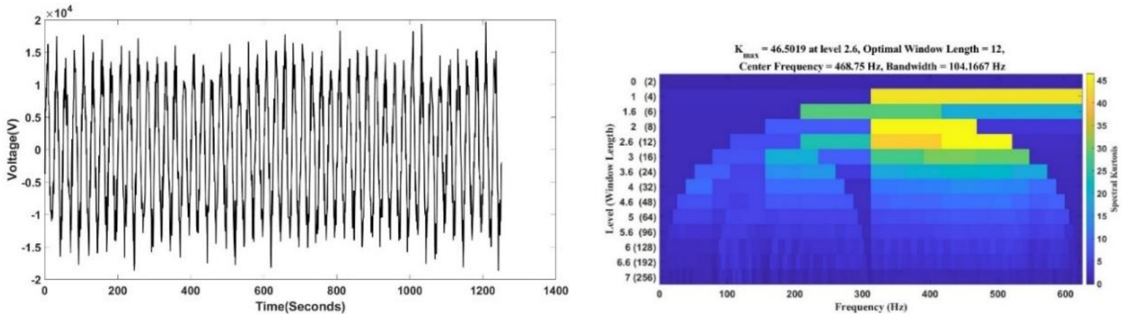

(a) (b)

Fig. 13. (a) Arc Voltage at various noisy conditions (10 dB), (b) Arc Kourtogram of Voltage at various noisy conditions (10 dB)

Table 10. Confusion matrix Under 25 dB SNR

		Predicted			Precision	Class index returned by classifier
		Zone 1	Zone2	Zone3		
Actual	Zone1	134	1	0	0.9925	0
	Zone2	0	134	1	0.9925	0
	Zone3	1	1	258	0.9923	3
					CA=97.24 %	

Table 11. Confusion matrix under 10 dB SNR

		Predicted			Precision	Class index returned by classifier
		Zone 1	Zone2	Zone3		
Actual	Zone1	134	1	0	0.9924	0
	Zone2	1	134	0	0.9924	0
	Zone3	1	1	258	0.9923	3
					CA=98.23%	

Table 12. Performance comparsion of the proposed method with previously published works

Method	Detection	Network	Noise (dB)	Accuracy (%)
WASVD+ k-NN [proposed methodology]	FD, classification and location	Radial, Meshed, with DG and Real Time	35dB 25dB 10dB	99.08
Tellegen's theorem [52]	Detection and classification	IEEE13 & 34	Not considered	98.5
Edge computing [53]	FD	Radial	Not considered	-
WT+SVM [54]	FD	Radial	Not considered	97.37
WT+kNN [55]	FD	Radial	Noise considered	99.25
WT+DT [56]	FD	Radial	Not considered	99.25
SWT +ANN [49]	Fault location	Radial	Not considered	100
PSO+ANN [57]	FD	Real time test feeder	Not considered	95.50
Sliding mode observer [51]	FD and classification	parallel multi-cell converter	Noise considered	-

6. Conclusion

For fault and zone classification in large power networks, an ANN built on the DWT has been presented. The network is divided into zones to make the entire power system observable and valuable, reduce computational strain, and save costs. NBPSO is a strategy for deciding the optimal placement of fault detectors in each zone. The ANN module is designed to pinpoint both the fault zone and the exact location within it. Additionally, the ANN is responsible for categorizing the types of faults that occur.In practical application, this method demonstrated its effectiveness by identifying a fault 100 kilometers away from fault detector 4 in zone 2. An L-G fault classification was achieved using data from the second fault detector. The accurate detection and categorization of the fault were made possible by the meticulous placement of fault locators, guided by NBPSO. The integration of ANN and DWT enhances the ability to detect and classify faults by providing detailed signal analysis. This combination allows for the recognition of patterns associated with different types of faults, making the system highly reliable. Dividing the network into zones not only makes the system easier to monitor but also reduces the computational load by processing data in smaller sections.The optimized placement of FDs ensures maximum coverage and efficiency in fault detection. By accurately pinpointing the fault zone and location, the system facilitates quick and effective responses to any issues. This method significantly improves the reliability and stability of the power network, ensuring a consistent and uninterrupted power supply. Through the use of advanced algorithms and precise fault locator placement, the proposed method offers a robust solution for FD and classification in large power networks.

Author Contributions: All authors contributed equally in this work. All authors have read and agreed to the published version of the manuscript.

Funding: This study is supported via funding from Prince sattam bin Abdulaziz University project number (PSAU/2024/R/1445).

Acknowledgement: This study is supported via funding from Prince sattam bin Abdulaziz University project number (PSAU/2024/R/1445).

Conflicts of Interest: The authors declare no conflict of interest.

References

[1] N. Benalia *et al.*, "Enhancing electric vehicle charging performance through series-series topology resonance-coupled wireless power transfer," *PLoS One*, vol. 19, no. 3, p. e0300550, 2024, https://doi.org/10.1371/journal.pone.0300550.

[2] M. Awad *et al.*, "A review of water electrolysis for green hydrogen generation considering PV/wind/hybrid/hydropower/geothermal/tidal and wave/biogas energy systems, economic analysis, and its application," *Alexandria Engineering Journal*, vol. 87, pp. 213-239, 2024, https://doi.org/10.1016/j.aej.2023.12.032.

[3] H. Abdelfattah *et al.*, "Optimal controller design for reactor core power stabilization in a pressurized water reactor: Applications of gold rush algorithm," *PLoS One*, vol. 19, no. 1, p. e0296987, 2024, https://doi.org/10.1371/journal.pone.0296987.

[4] M. Chebaani, M. M. Mahmoud, A. F. Tazay, M. I. Mosaad, and N. A. Nouraldin, "Extended Kalman Filter design for sensorless sliding mode predictive control of induction motors without weighting factor: An experimental investigation," *PLoS One*, vol. 18, no. 11, p. e0293278, 2023, https://doi.org/10.1371/journal.pone.0293278.

[5] S. R. K. Joga *et al.*, "Applications of tunable-Q factor wavelet transform and AdaBoost classier for identification of high impedance faults: Towards the reliability of electrical distribution systems," *Energy Exploration & Exploitation*, 2024, https://doi.org/10.1177/01445987241260949.

[6] B. S. Atia *et al.*, "Applications of Kepler Algorithm-Based Controller for DC Chopper: Towards Stabilizing Wind Driven PMSGs under Nonstandard Voltages," *Sustainability*, vol. 16, no. 7, p. 2952, 2024, https://doi.org/10.3390/su16072952.

[7] I. E. Maysse *et al*., "Nonlinear Observer-Based Controller Design for VSC-Based HVDC Transmission Systems Under Uncertainties," *IEEE Access*, vol. 11, pp. 124014-124030, 2023, https://doi.org/10.1109/ACCESS.2023.3330440.

[8] J. Jia, "Assessment of Short Circuit Power and Protection Systems for Future Low Inertia Power Systems," *DTU Orbit*, p. 184, 2018, https://orbit.dtu.dk/en/publications/assessment-of-short-circuit-power-and-protection-systems-for-futu.

[9] A. Raza, A. Benrabah, T. Alquthami, and M. Akmal, "A review of fault diagnosing methods in power transmission systems," *Applied Sciences*, vol. 10, no. 4, p. 1312, 2020, https://doi.org/10.3390/app10041312.

[10] N. F. Ibrahim *et al.*, "A new adaptive MPPT technique using an improved INC algorithm supported by fuzzy self-tuning controller for a grid-linked photovoltaic system," *PLoS One*, vol. 18, no. 11, p. e0293613, 2023, https://doi.org/10.1371/journal.pone.0293613.

[11] N. F. Ibrahim *et al*., "Operation of Grid-Connected PV System With ANN-Based MPPT and an Optimized LCL Filter Using GRG Algorithm for Enhanced Power Quality," *IEEE Access*, vol. 11, pp. 106859-106876, 2023, https://doi.org/10.1109/ACCESS.2023.3317980.

[12] F. M. Shakiba, S. M. Azizi, M. Zhou, and A. Abusorrah, "Application of machine learning methods in fault detection and classification of power transmission lines: a survey," *Artificial Intelligence Review*, vol. 56, pp. 5799-5836, 2023, https://doi.org/10.1007/s10462-022-10296-0.

[13] A. Prasad, J. Belwin Edward, and K. Ravi, "A review on fault classification methodologies in power transmission systems: Part-II," *Journal of Electrical Systems and Information Technology*, vol. 5, no. 1, pp. 61-67, 2018, https://doi.org/10.1016/j.jesit.2016.10.003.

[14] A. Prasad, J. Belwin Edward, and K. Ravi, "A review on fault classification methodologies in power

transmission systems: Part—I," *Journal of Electrical Systems and Information Technology*, vol. 5, no. 1, pp. 48-60, 2018, https://doi.org/10.1016/j.jesit.2017.01.004.

[15] M. M. Mahmoud, "Improved current control loops in wind side converter with the support of wild horse optimizer for enhancing the dynamic performance of PMSG-based wind generation system," *International Journal of Modelling and Simulation*, vol. 43, no. 6, pp. 952-966, 2023, https://doi.org/10.1080/02286203.2022.2139128.

[16] N. Tleis, "Power systems modelling and fault analysis: Theory and practice," *Academic Press*, 2019, https://doi.org/10.1016/C2017-0-02262-0.

[17] P. R. Chegireddy and R. Bhimasingu, "Fault location algorithm for multi-terminal transmission system," *Synchrophasor Technology: Real-time operation of power networks*, pp. 155-198, 2023, https://doi.org/10.1049/PBPO190E_ch7.

[18] A. M. Ewias *et al.*, "Advanced load frequency control of microgrid using a bat algorithm supported by a balloon effect identifier in the presence of photovoltaic power source," *PLoS One*, vol. 18, no. 10, p. e0293246, 2023, https://doi.org/10.1371/journal.pone.0293246.

[19] P. Balamurali Krishna and P. Sinha, "Detection of Power System Harmonics Using NBPSO Based Optimally Placed Harmonic Measurement Analyser Units," *2018 Second International Conference on Computing Methodologies and Communication (ICCMC)*, pp. 369-373, 2018, https://doi.org/10.1109/ICCMC.2018.8488114.

[20] M. Bakkar, S. Bogarra, F. Córcoles, A. Aboelhassan, S. Wang, and J. Iglesias, "Artificial Intelligence-Based Protection for Smart Grids," *Energies*, vol. 15, no. 13, p. 4933, 2022, https://doi.org/10.3390/en15134933.

[21] S. Mokred, Q. Lijun, and T. Khan, "Transient and Protection Performance of a Fixed Series Compensated 500 kV Transmission Line During Various Types of Faulty Conditions," *Journal of Electrical Engineering & Technology*, vol. 16, pp. 837–852, 2021, https://doi.org/10.1007/s42835-020-00646-9.

[22] N. F. Ibrahim *et al.*, "Multiport Converter Utility Interface with a High-Frequency Link for Interfacing Clean Energy Sources (PV\Wind\Fuel Cell) and Battery to the Power System: Application of the HHA Algorithm," *Sustainability*, vol. 15, no. 18, p. 13716, 2023, https://doi.org/10.3390/su151813716.

[23] B. Patel, "A new FDOST entropy based intelligent digital relaying for detection, classification and localization of faults on the hybrid transmission line," *Electric Power Systems Research*, vol. 157, pp. 39-47, 2018, https://doi.org/10.1016/j.epsr.2017.12.002.

[24] F. Lucas, P. Costa, R. Batalha, D. Leite, and I. Škrjanc, "Fault detection in smart grids with time-varying distributed generation using wavelet energy and evolving neural networks," *Evolving Systems*, vol. 11, pp. 165-180, 2020, https://doi.org/10.1007/s12530-020-09328-3.

[25] M. M. Hussein, T. H. Mohamed, M. M. Mahmoud, M. Aljohania, M. I. Mosaad, and A. M. Hassan, "Regulation of multi-area power system load frequency in presence of V2G scheme," *PLoS One*, vol. 18, no. 9, p. e0291463, 2023, https://doi.org/10.1371/journal.pone.0291463.

[26] A. Swetapadma and A. Yadav, "A Novel Decision Tree Regression-Based Fault Distance Estimation Scheme for Transmission Lines," *IEEE Transactions on Power Delivery*, vol. 32, no. 1, pp. 234-245, 2017, https://doi.org/10.1109/TPWRD.2016.2598553.

[27] N. S. Wani and R. P. Singh, "A novel approach for the detection, classification and localization of transmission lines faults using wavelet transform and Support Vector Machines classifier," *International Journal of Engineering & Technology*, vol. 7, no. 2, pp. 56-62, 2018, https://doi.org/10.14419/ijet.v7i2.17.11559.

[28] H. Boudjemai *et al.*, "Experimental Analysis of a New Low Power Wind Turbine Emulator Using a DC Machine and Advanced Method for Maximum Wind Power Capture," *IEEE Access*, vol. 11, pp. 92225-92241, 2023, https://doi.org/10.1109/ACCESS.2023.3308040.

[29] N. F. Ibrahim, A. Alkuhayli, A. Beroual, U. Khaled, and M. M. Mahmoud, "Enhancing the Functionality of a Grid-Connected Photovoltaic System in a Distant Egyptian Region Using an Optimized Dynamic Voltage Restorer : Application of Artificial Rabbits Optimization," *Sensors*, vol. 23, no. 16, p. 7146, 2023, https://doi.org/10.3390/s23167146.

[30] D. Guillen *et al.*, “Fault detection and classification in transmission lines based on a PSD index,” *IET Generation Transmission and Distribution*, vol. 12, no. 18, pp. 4070-4078, 2018, https://doi.org/10.1049/iet-gtd.2018.5062.

[31] S. AsghariGovar, P. Pourghasem, and H. Seyedi, “High impedance fault protection scheme for smart grids based on WPT and ELM considering evolving and cross-country faults,” *International Journal of Electrical Power & Energy Systems*, vol. 107, pp. 412–421, 2019, https://doi.org/10.1016/j.ijepes.2018.12.019.

[32] M. M. Mahmoud *et al.*, “Application of Whale Optimization Algorithm Based FOPI Controllers for STATCOM and UPQC to Mitigate Harmonics and Voltage Instability in Modern Distribution Power Grids,” *Axioms*, vol. 12, no. 5, p. 420, 2023, https://doi.org/10.3390/axioms12050420.

[33] A. H. Elmetwaly *et al.*, “Modeling, Simulation, and Experimental Validation of a Novel MPPT for Hybrid Renewable Sources Integrated with UPQC: An Application of Jellyfish Search Optimizer,” *Sustainability*, vol. 15, no. 6, p. 5209, 2023, https://doi.org/10.3390/su15065209.

[34] O. M. Kamel, A. A. Z. Diab, M. M. Mahmoud, A. S. Al-Sumaiti, and H. M. Sultan, “Performance Enhancement of an Islanded Microgrid with the Support of Electrical Vehicle and STATCOM Systems,” *Energies*, vol. 16, no. 4, p. 1577, 2023, https://doi.org/10.3390/en16041577.

[35] M. M. Mahmoud *et al.*, “Integration of Wind Systems with SVC and STATCOM during Various Events to Achieve FRT Capability and Voltage Stability: Towards the Reliability of Modern Power Systems,” *International Journal of Energy Research*, vol. 2023, no. 1, pp. 1-28, 2023, https://doi.org/10.1155/2023/8738460.

[36] A. D. S. Santos, L. T. Faria, M. L. M. Lopes, A. D. P. Lotufo, and C. R. Minussi, “Efficient Methodology for Detection and Classification of Short-Circuit Faults in Distribution Systems with Distributed Generation,” *Sensors*, vol. 22, no. 23, p. 9418, 2022, https://doi.org/10.3390/s22239418.

[37] M. M. Mahmoud *et al.*, “Voltage Quality Enhancement of Low-Voltage Smart Distribution System Using Robust and Optimized DVR Controllers : Application of the Harris Hawks Algorithm,” *International Transactions on Electrical Energy Systems*, vol. 2022, no. 1, pp. 1-18, 2022, https://doi.org/10.1155/2022/4242996.

[38] M. M. Zaben, M. Y. Worku, M. A. Hassan and M. A. Abido, "Machine Learning Methods for Fault Diagnosis in AC Microgrids: A Systematic Review," *IEEE Access*, vol. 12, pp. 20260-20298, 2024, https://doi.org/10.1109/ACCESS.2024.3360330.

[39] M. M. Mahmoud, M. Khalid Ratib, M. M. Aly, and A. M. M. Abdel-Rahim, “Wind-driven permanent magnet synchronous generators connected to a power grid: Existing perspective and future aspects,” *Wind Engineering*, vol. 46, no. 1, pp. 189-199, 2022, https://doi.org/10.1177/0309524X211022728.

[40] S. R. K. Joga, P. Sinha, and M. K. Maharana, “Genetic Algorithm and Graph Theory Approach to Select Protection Zone in Distribution System,” *Lecture Notes in Electrical Engineering*, vol. 688, pp. 165-174, 2021, https://doi.org/10.1007/978-981-15-7241-8_13.

[41] H. Shayeghi, B. Sobhani, E. Shahryari, and A. Akbarimajd, “Optimal neuro-fuzzy based islanding detection method for Distributed Generation,” *Neurocomputing*, vol. 177, pp. 478-488, 2016, https://doi.org/10.1016/j.neucom.2015.11.056.

[42] K. Andanapalli, N. Shaik, S. Vudumudi, and B. C. Yenugu, “Fault detection, classification and location on transmission lines using fundamental phasor based approach,” *International Journal of Recent Technology and Engineering*, vol. 8, no. 1S3, pp. 288–293, 2019, https://www.ijrte.org/wp-content/uploads/papers/v8i1S3/A10510681S319.pdf.

[43] A. R. Adly, R. A. El Sehiemy, M. A. Elsadd, and A. Y. Abdelaziz, “A novel wavelet packet transform based fault identification procedures in HV transmission line based on current signals,” *International Journal of Applied Power Engineering*, vol. 8, no. 1, pp. 11-21, 2019, http://doi.org/10.11591/ijape.v8.i1.pp11-21.

[44] F. Yalçin and Y. Yildirim, “A Study of Symmetrical and Unsymmetrical Short Circuit Fault Analyses in Power Systems,” *Sakarya University Journal of Science*, vol. 23, no. 5, pp. 879-895, 2019, https://doi.org/10.16984/saufenbilder.540294.

[45] D. K. J. S. Jayamaha, N. W. A. Lidula and A. D. Rajapakse, "Wavelet-Multi Resolution Analysis Based ANN Architecture for Fault Detection and Localization in DC Microgrids," *IEEE Access*, vol. 7, pp. 145371-145384, 2019, https://doi.org/10.1109/ACCESS.2019.2945397.

[46] V. Ashok and A. Yadav, "A real-time fault detection and classification algorithm for transmission line faults based on MODWT during power swing," *International Transactions on Electrical Energy Systems*, vol. 30, no. 1, p. e12164, 2020, https://doi.org/10.1002/2050-7038.12164.

[47] B. Y. Vyas, R. P. Maheshwari, and B. Das, "Versatile relaying algorithm for detection and classification of fault on transmission line," *Electric Power Systems Research*, vol. 192, p. 106913, 2021, https://doi.org/10.1016/j.epsr.2020.106913.

[48] M. Guo, X. Zeng, D. Chen and N. Yang, "Deep-Learning-Based Earth Fault Detection Using Continuous Wavelet Transform and Convolutional Neural Network in Resonant Grounding Distribution Systems," *IEEE Sensors Journal*, vol. 18, no. 3, pp. 1291-1300, 2018, https://doi.org/10.1109/JSEN.2017.2776238.

[49] Y. Sun, Y. Chang, S. Yang, and F. Wang, "Dynamic niching particle swarm optimization with an external archive-guided mechanism for multimodal multi-objective optimization," *Information Sciences*, vol. 653, p. 119794, 2024, https://doi.org/10.1016/j.ins.2023.119794.

[50] N. B. Roy and K. Bhattacharya, "Application of Signal Processing Tools and Artificial Neural Network in Diagnosis of Power System Faults," *CRC Press*, 2021, https://doi.org/10.1201/9780367431143.

[51] M. Misiti, Y. Misiti, G. Oppenheim, and J. Poggi, "Wavelet Toolbox TM 4 User ' s Guide," *MathWorks Inc*, 1996, http://feihu.eng.ua.edu/NSF_TUES/w7_1a.pdf

[52] M. Zhang, Z. Zhang, Z. Li, J. Wang, Y. Zhang and S. Liu, "A Simple and Effective Open-Circuit-Fault Diagnosis Method for Grid-Tied Power Converters—A New Technique Based on Tellegen's Theorem," *IEEE Journal of Emerging and Selected Topics in Power Electronics*, vol. 11, no. 2, pp. 2203-2213, 2023, https://doi.org/10.1109/JESTPE.2022.3218171.

[53] S. Netsanet, D. Zheng, Z. Wei, and G. Teshager, "Cognitive Edge Computing–Based Fault Detection and Location Strategy for Active Distribution Networks," *Frontiers in Energy Research*, vol. 10, p. 826915, 2022, https://doi.org/10.3389/fenrg.2022.826915.

[54] A. Ahmadi, E. Aghajari, and M. Zangeneh, "High-impedance fault detection in power distribution grid systems based on support vector machine approach," *Electrical Engineering*, vol. 104, pp. 3659-3672, 2022, https://doi.org/10.1007/s00202-022-01544-1.

[55] M. Mishra and R. R. Panigrahi, "Advanced signal processing and machine learning techniques for voltage sag causes detection in an electric power system," *International Transactions on Electrical Energy Systems*, vol. 30, no. 1, p. e12167, 2020, https://doi.org/10.1002/2050-7038.12167.

[56] K. Moloi and I. Davidson, "High Impedance Fault Detection Protection Scheme for Power Distribution Systems," *Mathematics*, vol. 10, no. 22, p. 4298, 2022, https://doi.org/10.3390/math10224298.

[57] S. C. Kim, P. Ray, and S. R. Salkuti, "Islanding detection in a distribution network with distributed generators using signal processing techniques," *International Journal of Power Electronics and Drive System*, vol. 11, no. 4, pp. 2099-2106, 2020, http://doi.org/10.11591/ijpeds.v11.i4.pp2099-2106.